

Acetylcholinesterase Adsorption on Modified Gold: Effect of Surface Chemistry on Enzyme Binding and Activity

Joshua M. Correira, Diane E. Madeksho, and Lauren J. Webb*



Cite This: <https://doi.org/10.1021/acs.langmuir.3c00648>



Read Online

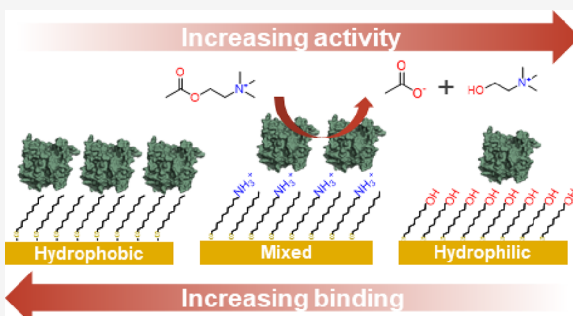
ACCESS |

Metrics & More

Article Recommendations

Supporting Information

ABSTRACT: Surface chemistry plays a crucial role in the performance of biosensors and biocatalysts, where enzymes directly interact with a solid support. In this work, we investigated the effect of surface charge and hydrophobicity on the binding and activity of acetylcholinesterase (AChE) following direct adsorption to modified gold surfaces. Surface modifications included self-assembled monolayers (SAMs) terminated with $-COO^-$, $-NH_3^+$, $-OH$, and $-CH_3$ functional groups at varying mole %. We also investigated the effects of positively and negatively charged helical peptides covalently coupled to the SAM. Using spectroscopic ellipsometry, we measured the surface concentration of AChE on each modified surface after 1 h of adsorption. We found that surface concentration was directly proportional to surface hydrophobicity ($r = 0.76$). The highest binding was observed on the more hydrophobic surfaces. We also measured the specific activity of AChE on each surface using a colorimetric assay and found that activity was inversely proportional to surface hydrophobicity ($r = -0.71$). The highest activity was observed on the more hydrophilic surfaces. Plotting specific activity versus surface concentration showed a similar relationship, with the highest activity observed at low AChE densities (~20% of a monolayer) on surfaces terminated with 50% $-COO^-$ or $-NH_3^+$ and 50% $-CH_3$ functional groups. Interestingly, this is similar to the approximate composition of hydrophobic versus hydrophilic amino acid residues on the surface of AChE. These surfaces also exhibited the highest total activity: a ~100% improvement over bare gold due to a combination of moderate binding and high activity retention. This work highlights the importance of developing new attachment strategies beyond direct adsorption that promote, tune, and optimize both high binding and high activity retention.



INTRODUCTION

Enzymes are the basis for biosensors and biocatalysts, where they are immobilized on a solid support to transduce a biochemical signal or generate chemical products. To improve the sensitivity and turnover rate of biosensors and biocatalysts, the number and activity of individual catalytic sites need to be improved. The number of sites can be optimized by increasing the surface area of the solid support or by increasing the binding and surface density of the immobilized enzyme. The activity of individual sites is less straightforward to improve. Ideally, individual enzymes are as active on the surface as they are in solution. However, this is often not the case due to direct interactions between the enzyme and the surface, resulting in denaturing structural changes, less active conformations, or altered structural and conformational dynamics and blocking of the active site.^{1–10} The surface chemistry of the solid support plays a critical role in determining binding and activity by controlling the enzyme–surface interactions. In general, surfaces with hydrophobic functional groups tend to be detrimental to enzyme activity due to hydrophobic enzyme–surface interactions, dehydration, and altered structural and conformational dynamics, which can favor unfolded, misfolded, and less active conformations of the

enzyme. These surfaces also tend to have higher binding and surface density due to stronger enzyme–surface interactions. Conversely, surfaces with hydrophilic functional groups tend to be significantly less detrimental to enzyme activity but exhibit lower binding due to weaker enzyme–surface interactions.

Surface chemistry can be controlled by modifying the solid support with various functional molecules. A common method is the use of self-assembled monolayers (SAMs) containing a reactive head group that binds to the substrate, a spacer (commonly an alkane chain), and a tail group containing functional or reactive groups that determine the surface properties.¹¹ SAMs can be formed on a variety of substrates including metals, oxides, glasses, and silicon. Gold is one of the most commonly used substrates to form SAMs through the use of alkanethiols due to its simplicity. The sulfur head group

Received: March 8, 2023

Revised: June 15, 2023

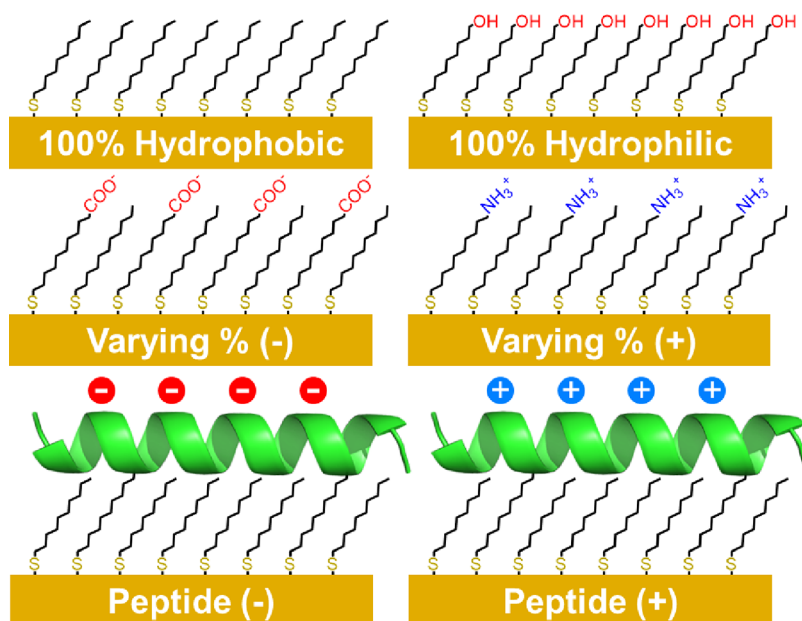


Figure 1. Schematic of modified surfaces prepared for AChE adsorption. Varying % charged SAMs include 30/70% charged/hydrophobic, 50/50% charged/hydrophobic, and 100% charged. The actual thiol lengths used are described in the text.

binds to the gold, van der Waals interactions between the alkane chains cause the thiol to stand upright, and the terminal functional group is displayed on the surface of the monolayer. A variety of thiols with hydrophobic, hydrophilic, charged, or reactive groups can be used to modify the surface chemistry of the substrate and provide a platform for further chemical modification. Mixtures of thiols can also be formed on the surface through co-adsorption or by exchange.¹²

In this work, we have generated a variety of hydrophobic, hydrophilic, and mixed charged SAMs on planar gold (Figure 1) to investigate how surface chemistry, specifically charge and hydrophobicity, affects the binding and activity of the enzyme acetylcholinesterase (AChE) immobilized through direct adsorption. We have also extended this to two biomimetic surfaces consisting of a positively or negatively charged helical peptide covalently bound to the SAM. We chose to use SAMs terminated with $-\text{CH}_3$, $-\text{OH}$, $-\text{COO}^-$, and $-\text{NH}_3^+$ functional groups to introduce hydrophobic, hydrophilic, negatively charged, and positively charged groups, respectively. SAMs containing mixtures of varying positive or negative charges were generated in ratios of 30/70% charged/hydrophobic, 50/50% charged/hydrophobic, and 100% charged. The hydrophobicity of each modified surface was estimated by wettability using contact angle goniometry.¹³ AChE was then adsorbed onto the surface, its binding was measured using spectroscopic ellipsometry (SE), and its activity was measured using a colorimetric assay. AChE was chosen because we have previously shown that it is only $\sim 10\%$ active following adsorption on bare gold. However, this active fraction remained functional for up to 100 days, prompting us to investigate alternative surface chemistry strategies that both improve AChE binding and retain activity over time.¹⁴ These results will inform the development of new surface materials and enzyme immobilization methods that promote high binding and high activity retention for use in biosensors and biocatalysts.

MATERIALS AND METHODS

Modified Surface Preparation. Gold surfaces were prepared as described previously.¹⁴ SAMs were prepared by immersing the gold surface in an ethanolic thiol solution. The following SAMs were prepared: 100% hydrophobic (1 mM decanethiol, 24 h), 100% hydrophilic (5 mM 11-mercapto-1-undecanol, 24 h), 30% negatively charged (0.5 mM 11-mercapto-1-undecanoic acid, 0.5 mM decanethiol, 48 h), 30% positively charged (0.5 mM 8-amino-1-octanethiol, 0.5 mM octanethiol, 48 h), 50% negatively charged (0.75 mM 11-mercapto-1-undecanoic acid, 0.25 mM decanethiol, 48 h), 50% positively charged (0.75 mM 8-amino-1-octanethiol, 0.25 mM octanethiol), 100% negatively charged (5 mM 11-mercapto-1-undecanoic acid, 24 h), and 100% positively charged (5 mM 8-amino-1-octanethiol, 24 h). The concentrations used here have been reported previously, as the composition of mixed thiol solutions may not directly reflect the resulting mixed SAM composition.¹² In general, the equilibrium composition of mixed SAMs tends to favor thiols with nonpolar tail groups, which pack more efficiently than polar tail groups, so the solution composition was adjusted accordingly. Mixed SAM compositions were verified using X-ray photoelectron spectroscopy (XPS) (Figures S1 and S2).

Peptide-functionalized surfaces were prepared as described previously.¹⁵ Briefly, 25% Br-terminated SAMs were prepared (0.25 mM 11-bromo-1-undecanethiol, 0.75 mM decanethiol, 24 h) and reacted with saturated sodium azide in dimethylformamide to form 25% N_3 -terminated SAMs. These SAMs then underwent copper-catalyzed azide–alkyne cycloaddition (“click”) chemistry with either a positively charged lysine-containing peptide (LKKLXKKLLKKLKKXLKKL) or a negatively charged glutamate-containing peptide (LEELXEEELLEELLEEXLEEL), where X represents the alkyne-containing propargylglycine residue. The positively charged peptide was reacted in the following conditions: 30 μM peptide, 180 μM tris[(1-benzyl-1H-1,2,3-triazol-4-yl)methyl]amine, 1.2 mM sodium ascorbate, and 180 μM copper(II) sulfate in a 2:1 mixture of *tert*-butanol and water at 70 °C for 6 h. The negatively charged peptide was reacted in the following conditions: 120 μM peptide, 1.2 mM tris(3-hydroxypropyltriazolylmethyl)amine, 5 mM sodium ascorbate, and 240 μM copper(II) sulfate in phosphate-buffered saline at room temperature for 48 h.

Contact Angle Goniometry. Water contact angle measurements were performed on each modified surface using an FTA200 contact angle goniometer. High-purity water was automatically dispensed

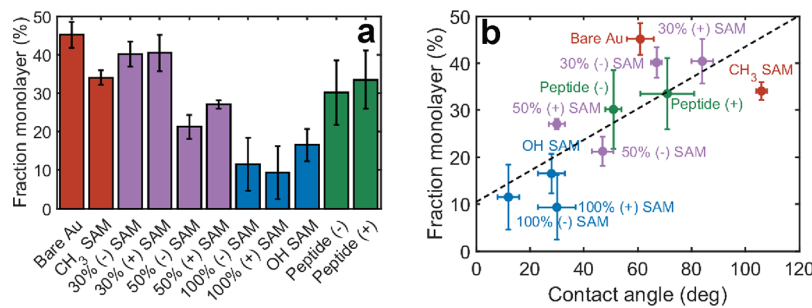


Figure 2. (a) Surface density of AChE adsorbed on hydrophobic (red), mixed (purple), hydrophilic (blue), and peptide (green) surfaces reported as the fraction of a fully packed monolayer. (b) Fraction monolayer plotted versus the water contact angle of each surface. The dashed line represents a linear fit ($r = 0.76$) as a visual guide to show the general trend. The vertical error bars represent the standard deviation of three replicate samples. The horizontal error bars represent the standard deviation of three measurements on four replicate samples.

from a syringe to create a droplet that was placed onto the surface. Contact angles were measured using a camera and calculated using the instrument's FTA32 software by an automatic nonspherical fit to the liquid–vapor interface.

AChE Activity Assay. AChE from electric eel (*Electrophorus electricus*) was purchased from MilliporeSigma, purified by size exclusion chromatography, adsorbed onto each modified surface described above, and characterized as described previously.¹⁴ Briefly, the activity of adsorbed AChE was measured by a colorimetric assay adapted from Ellman using acetylthiocholine (ATCh) as the substrate and 5,5-dithio-bis-(2-nitrobenzoic acid) (DTNB) as a dye.¹⁶ AChE-coated surfaces were placed in vials containing 3 mL of 100 mM sodium phosphate (pH 8), 66.7 μ M DTNB, and concentrations of ATCh ranging from 125 μ M to 6 mM. The assay was allowed to progress untouched for 2 min. The vial was then mixed and 2 mL of liquid was removed to stop the assay and measure its absorbance at 412 nm ($\epsilon = 1.36 \times 10^4 \text{ M}^{-1} \text{ cm}^{-1}$). Specific activity was reported as 1 U $\text{mg}^{-1} = 1 \mu\text{mol}$ of ATCh hydrolyzed per minute per milligram of AChE present.

Spectroscopic Ellipsometry. The surface concentration and density of AChE on each modified surface were determined by SE as described previously using a commercial liquid cell mounted on an M-2000 spectroscopic ellipsometer (J.A. Woollam) in 100 mM sodium phosphate buffer (pH 8) to ensure that AChE remained hydrated.¹⁴ SE data were fit to a model consisting of a bare gold surface with a single transparent film on top describing the SAM with adsorbed AChE. Due to thickness–index correlation in ultrathin films, SE is not sensitive to both thickness and refractive index simultaneously but is sensitive to their product (optical thickness). For modeling purposes, the refractive index of the film was held constant ($n = 1.4788$ at 589.3 nm), despite the difference in the refractive index of SAMs and protein films, and only thickness was fit to give a unique solution.¹⁷ This results in an accurate optical thickness but a measured film thickness that may not reflect the true film thickness. Consequently, a single film was used for analysis instead of two films for the SAM and AChE separately, as they are treated as optically identical by fixing the refractive index and can simply be combined. Thus, the measured film thickness was attributed to the sum of the individual SAM and AChE films. To determine the thickness of the AChE film alone, the thickness of the SAM was measured separately prior to AChE adsorption and subtracted. The AChE surface concentration was then calculated using the de Feijter equation shown below in eq 1:

$$\Gamma = \frac{d(n - n_0)}{M_w(dn/dc)} \quad (1)$$

where Γ is the surface concentration in mol cm^{-2} , d is the measured thickness of the AChE film in cm , n is the fixed refractive index of the film ($n = 1.4788$ at 589.3 nm), n_0 is the refractive index of the ambient buffer ($n_0 = 1.334$ at 589.3 nm), M_w is the molecular weight of AChE (69,139 g mol^{-1} for the monomer), and dn/dc is the refractive index increment in $\text{cm}^3 \text{ g}^{-1}$ describing how n varies with AChE concentration.¹⁸ The dn/dc was calculated for AChE to be 0.195

$\text{cm}^3 \text{ g}^{-1}$ from its amino acid sequence as described previously.¹⁹ Conveniently, the numerator contains the optical thickness, allowing for an accurate calculation of surface concentration, despite the potentially inaccurate measured thickness and fixed refractive index. Surface density, or the fraction of the surface occupied by AChE, was calculated from surface coverage by dividing the volume occupied by AChE molecules on the surface by the total volume of the film, shown below in eq 2:

$$\theta = \frac{V_m M_w \Gamma}{d} \times 100 \quad (2)$$

where V_m is the molecular volume of AChE in $\text{cm}^3 \text{ g}^{-1}$, M_w is the molecular weight of AChE in g mol^{-1} , Γ is the calculated surface concentration in mol cm^{-2} , and d is the film thickness in cm . In this case, the d corresponds to the diameter of AChE, not the measured film thickness. The V_m was calculated as described previously.¹⁴ Surface density was then converted into the fraction of a fully packed monolayer by dividing by the maximal packing possible (74% density, based on spheres packing into a box).

RESULTS AND DISCUSSION

AChE Binding. AChE was adsorbed onto the modified surfaces described above and its binding was measured to examine the effects of surface hydrophobicity and charge. These surfaces were 100% hydrophobic ($-\text{CH}_3$), 100% hydrophilic ($-\text{OH}$), 30% positively ($-\text{NH}_3^+$) or negatively ($-\text{COO}^-$) charged, 50% positively or negatively charged, 100% positively or negatively charged, and positively or negatively charged peptide-functionalized SAMs. The surface concentration and surface density of AChE were measured after 1 h of adsorption on each surface by SE. Surface density was divided by the maximum packing possible (74%) to determine the fraction of a fully packed monolayer (Figure 2a). The bare Au surface showed the highest AChE binding, and the 100% charged and $-\text{OH}$ SAMs showed the lowest binding. In general, it was observed that more hydrophobic surfaces exhibited higher AChE binding and more hydrophilic surfaces exhibited lower AChE binding. To quantify this, water contact angles were measured on each surface as a measure of surface hydrophobicity, with high angles corresponding to hydrophobic surfaces and low angles corresponding to hydrophilic surfaces. The fraction monolayer on each surface was plotted versus the water contact angle of that surface (Figure 2b), with a linear fit used as a visual guide. Bare Au was not included in the linear fit because its exceedingly high surface density may partially be due to the formation of gold–sulfur bonds through surface cysteine residues in AChE, a process that does not occur as readily in the presence of a SAM blocking layer. For the other surfaces, where physical adsorption is the dominant

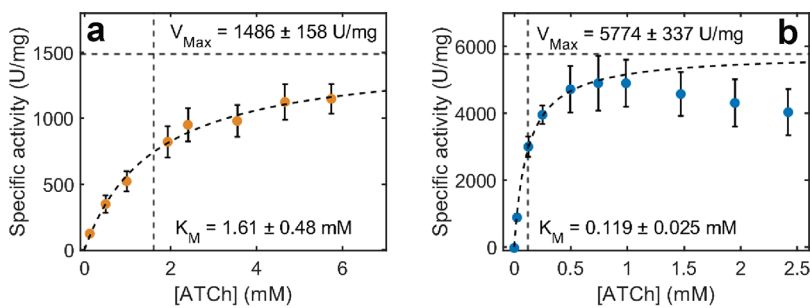


Figure 3. Representative example of Michaelis–Menten kinetics of AChE (a) adsorbed on a 100% negatively charged SAM compared to (b) native in aqueous solution. The error bars represent the standard deviation of three replicate samples. The dashed curve shows fit to the Michaelis–Menten equation (eq 3). The vertical dashed line indicates the K_M , and the horizontal dashed line indicates the V_{Max} .

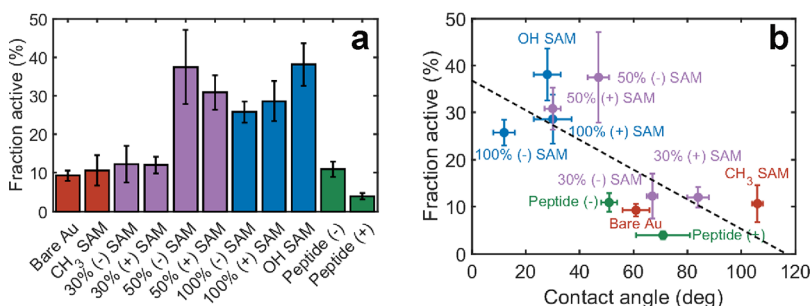


Figure 4. (a) Fraction of active AChE adsorbed on hydrophobic (red), mixed (purple), hydrophilic (blue), and peptide (green) surfaces. (b) Fraction active plotted versus the water contact angle of each surface. The dashed line represents a linear fit ($r = -0.71$) as a visual guide to show the general trend. The vertical error bars represent the 95% confidence interval of V_{Max} from the fit to the Michaelis–Menten equation (eq 3), normalized to fraction active. The horizontal error bars represent the standard deviation of three measurements on four replicate samples.

process governing binding, there is a direct relationship between surface hydrophobicity and surface density ($r = 0.76$). The most hydrophilic surfaces (100% charged and $-OH$ SAMs) exhibited the lowest AChE binding, and the more hydrophobic surfaces ($-CH_3$ SAM, 30% charged SAMs) exhibited the highest binding. Additionally, there did not appear to be an effect of the sign of the charge on binding, despite the fact that AChE carries a net negative charge (-9 per monomer) and has a large molecular dipole (~ 1000 D per monomer).^{20,21}

The direct relationship between surface density and surface hydrophobicity of adsorbed enzymes has been observed previously.^{22–27} This suggests that to generate a surface with a high density of bound enzymes, a hydrophobic substrate should be used. Surface density is important in the context of biosensors and biocatalysts because a higher surface density generates more catalytic sites on the surface, which results in improved sensitivity and performance. This is because enzyme activity is directly proportional to enzyme concentration. However, beyond surface density, enzyme activity is also affected by the surface chemistry of the substrate being used and must be considered before selecting a substrate material.

AChE Activity. The activity of AChE on each modified surface was measured (Figures S3–S13) and compared to the activity of native AChE in solution using the spectroscopic assay described above. This was done to examine how surface hydrophobicity and charge affect adsorbed enzyme activity. To do this, activity was measured on the surface at ATCh concentrations ranging from $125 \mu\text{M}$ to 6 mM and in solution at ATCh concentrations ranging from $25 \mu\text{M}$ to 2.5 mM . Activity measurements are reported as specific activity normalized by the mass of AChE present on the surface or

in solution. An example of these results is shown in Figure 3a for AChE immobilized on a 100% negatively charged SAM and Figure 3b for native AChE in solution. The data were fit to the Michaelis–Menten equation, represented by the dashed line, shown below in eq 3:

$$\nu = \frac{V_{\text{Max}}[S]}{K_M + [S]} \quad (3)$$

where ν is the observed rate of reaction, V_{Max} is the maximal rate of reaction, $[S]$ is the ATCh concentration, and K_M is the Michaelis constant.²⁸

During catalysis, two main processes occur that contribute to the observed rate: diffusion of ATCh to the active site and hydrolysis of ATCh by AChE into acetate and choline. Figure 3a,b shows that at lower ATCh concentrations, activity increased more rapidly with increasing ATCh concentration. This is because the rate-limiting step of catalysis in this region is diffusion of ATCh to the active site. When AChE was diffusion limited, adding more ATCh increased the rate of mass transport to the active site and increased the observed rate of reaction. Eventually, at high enough ATCh concentrations, the rate plateaued. This is because the rate of mass transport of ATCh to the active site overcame the rate of hydrolysis of ATCh by AChE, which was then the rate-limiting step, and AChE was kinetically limited. In this region, ν approached V_{Max} and the true catalytic activity of AChE in the absence of diffusion limitations became apparent. This is important because diffusion to an active site on a surface occurs in two dimensions (planar diffusion) and is slower than diffusion to an active site in solution, which occurs in three dimensions (spherical diffusion). In general, K_M can be used as

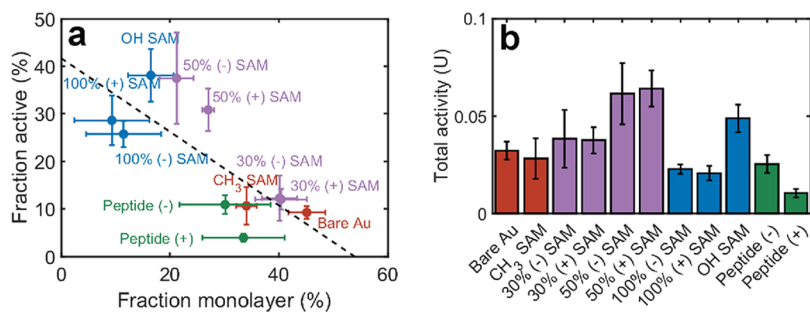


Figure 5. (a) Activity versus surface density of AChE adsorbed on hydrophobic (red), mixed (purple), hydrophilic (blue), and peptide (green) surfaces. The dashed line shows a linear fit ($r = -0.76$) as a visual guide to show the general trend. (b) Total activity of AChE adsorbed on various surfaces. The vertical error bars represent the 95% confidence interval of V_{Max} from the fit to the Michaelis–Menten equation (eq 3). The horizontal error bars represent the standard deviation of three replicate samples.

a measure of the extent of diffusion limitation of a system and tends to be higher on surfaces by an order of magnitude.

In Figure 3, the V_{Max} of adsorbed AChE was compared to the V_{Max} of native aqueous AChE to determine what fraction of AChE remained active on the surface following adsorption. In this case, AChE was $25.7 \pm 2.7\%$ active following adsorption on a 100% negatively charged SAM compared to native in solution. This comparison was done for each modified surface and can be seen in Figure 4a. In general, it was observed that AChE adsorbed on more hydrophobic surfaces was less active than on hydrophilic surfaces. This observation is due to interactions with hydrophobic surfaces that can result in denaturing structural changes, favoring less active conformations, and altered structural and conformational dynamics leading to frequent blocking of the active site. However, this inverse relationship, shown in Figure 4b, was not as strong ($r = -0.71$) as the direct relationship between surface density and hydrophobicity. This is because activity loss following adsorption is a more complex process with many contributing factors including surface hydration, interfacial ionic strength and pH, enzyme structure and orientation, and structural and conformational dynamics. In particular, it has been shown that enzymes exhibit similar levels of denaturation on hydrophobic and hydrophilic surfaces but are much more dynamic on hydrophobic surfaces, which may explain this observed trend.¹⁰ Increased conformational dynamics can lead to more frequent blocking of the active site and lower residence times in folded or active states. K_{M} was found to be slightly lower on the most hydrophilic surfaces (Figure S14), suggesting that the active site of AChE is more accessible for catalysis, possibly due to slower conformational dynamics.

Despite this, hydrophilic surfaces performed consistently better than hydrophobic surfaces, as has been shown previously.^{5,22} Two exceptions to this were the positively and negatively charged peptides, which performed poorly despite their intermediate hydrophobicity, possibly owing to the presence of residual aggregates of reagents from the click reaction drastically altering the local surface environment. This could be alleviated in the future by using copper-less click chemistry strategies, such as strain-promoted azide–alkyne click chemistry. Interestingly, the best performers were the 50% charged SAMs, followed by the -OH SAM and 100% charged SAMs. This suggests that a mixture of charged, hydrophilic, and hydrophobic characters on the surface is optimal for activity retention following adsorption. This aligns with the composition of residues on the surface of the enzyme, which is generally around 50% hydrophilic/50% hydrophobic

for most proteins, including AChE.^{29,30} Again, there did not appear to be any effect of surface charge sign on activity, since both negatively and positively charged counterparts performed similarly. This is surprising, given that AChE has a large molecular dipole, which has been shown to affect enzyme orientation on positively versus negatively charged surfaces.^{2,21,31–33} This suggests that AChE activity, at least for ATCh hydrolysis and colorimetric detection, is independent of its orientation on the surface. This could differ for electrochemical detection methods, where diffusion and electron transfer to the electrode may be sensitive to orientation. Based on activity measurements alone, a hydrophilic surface (50% or higher in polar groups) should be used to generate a surface with the best performance. However, both surface density and activity should be considered before selecting a substrate material.

Optimizing Total Activity. Given the results from AChE binding and activity measurements on the modified surfaces, we can now make informed decisions about how to design a substrate material to optimize the total activity of the system. Total activity refers to the total amount of the substrate reacted per unit time on the surface and is a product of the amount of the enzyme present (surface density) and the individual enzyme activity (specific activity). Optimally, the system will have high surface density and high specific activity, resulting in a high total activity. In biosensors and biocatalysts, this increases the number of catalytic sites as well as the activity of each individual catalytic site, resulting in improved sensitivity and performance.

We determined the performance of each modified surface used here first by plotting the fraction of active AChE versus the surface density, as shown in Figure 5a. An optimal surface would reside in the upper-right corner of the figure, at high activity and high surface density. Unfortunately, as the surface density increased, the activity decreased because of the increasing surface hydrophobicity, as discussed above. We also looked at the total activity, as shown in Figure 5b. The best-performing surfaces, again, were the 50% charged SAMs because of their high binding and high specific activity. Interestingly, the 100% charged SAMs had lower total activity than the less individually active bare Au, -CH₃ SAM, and 30% charged SAMs because of the significantly lower binding observed on the 100% charged SAMs. This highlights an important consideration when optimizing a specific biosensor: simply measuring the raw total activity of a surface is insufficient for understanding performance in the absence of measuring surface binding. Based on Figure 5b, it appeared

that using a 100% charged SAM was worse than using bare Au. However, upon performing the analysis in this work, it became clear that the total activity on 100% charged SAMs could potentially be improved by increasing AChE binding because it already has high specific activity. This could be done in several ways, for example, by increasing AChE concentration in solution during binding or by covalently linking the enzyme to the surface.

This work also illuminates an inherent contradiction with the adsorption binding strategy used here. To optimize the total activity of a system, high specific activity and high binding are desired. However, to achieve high binding, a hydrophobic surface is required, which is detrimental to specific activity. This is because the driving force for adsorption is displacement of an equal volume of water at the solution–surface interface. Hydrophobic surfaces are easily dehydrated, and adsorption readily occurs. Hydrophilic surfaces are less easily dehydrated due to strong surface–water interactions, and adsorption occurs less readily.^{23,34,35} Thus, to optimize the total activity of a system with high binding and high specific activity, direct adsorption should be avoided. Instead, an alternative attachment strategy, such as attachment through covalent or affinity linkages, could be used to promote higher binding on a hydrophilic surface that will preserve specific activity. We are exploring that strategy in our laboratory and will report on it in future work.

CONCLUSIONS

In this work, we have characterized the activity and binding of AChE to a combination of hydrophobic, hydrophilic, charged, and biomimetic modified gold surfaces through direct adsorption. We found that hydrophobic surfaces promote high levels of binding, up to ~50% of a monolayer, at the cost of activity, with reductions down to ~10% native levels. Conversely, we found that hydrophilic surfaces promote high levels of activity, up to ~40% native levels, at the cost of binding, down to ~10% of a monolayer. To optimize the total activity of the surface, a combination of hydrophobic and hydrophilic functional groups should be used to promote high levels of activity while still offering moderate levels of binding. Unfortunately, we found that the use of a biomimetic peptide layer hindered activity, despite its mixed hydrophobic/hydrophilic character. This was possibly due to residual aggregates of reagents from the click reaction on the surface and may be improved by the use of copper-less click chemistry. Ultimately, we found that generating a surface that promotes high levels of binding and high levels of activity through direct adsorption is difficult because of the nature of enzyme–surface interactions. We plan to use these findings to inform future experiments on designing surface materials and immobilization strategies beyond direct adsorption where both binding and activity can be maximized.

ASSOCIATED CONTENT

Supporting Information

The Supporting Information is available free of charge at <https://pubs.acs.org/doi/10.1021/acs.langmuir.3c00648>.

XPS spectra of the C 1s region of varying compositions of positively and negatively charged mixed SAMs, Michaelis–Menten kinetics of AChE adsorbed on each modified surface, and comparison of K_M on each modified surface (PDF)

AUTHOR INFORMATION

Corresponding Author

Lauren J. Webb – Department of Chemistry, Texas Materials Institute, and Interdisciplinary Life Sciences Program, The University of Texas at Austin, Austin, Texas 78712-1224, United States;  orcid.org/0000-0001-9999-5500; Email: lwebb@cm.utexas.edu

Authors

Joshua M. Correira – Department of Chemistry, Texas Materials Institute, and Interdisciplinary Life Sciences Program, The University of Texas at Austin, Austin, Texas 78712-1224, United States;  orcid.org/0000-0002-2971-4619

Diane E. Madeksho – Department of Chemistry, Texas Materials Institute, and Interdisciplinary Life Sciences Program, The University of Texas at Austin, Austin, Texas 78712-1224, United States;  orcid.org/0000-0003-3138-9664

Complete contact information is available at: <https://pubs.acs.org/10.1021/acs.langmuir.3c00648>

Notes

The authors declare no competing financial interest.

ACKNOWLEDGMENTS

This work was supported by the National Science Foundation (grant nos. CHE-1807215 and CHE-2203414). We gratefully acknowledge the use of facilities at the Texas Materials Institute at The University of Texas at Austin.

REFERENCES

- (1) Badieyan, S.; Wang, Q.; Zou, X.; Li, Y.; Herron, M.; Abbott, N. L.; Chen, Z.; Marsh, E. N. G. Engineered Surface-Immobilized Enzyme That Retains High Levels of Catalytic Activity in Air. *J. Am. Chem. Soc.* **2017**, *139*, 2872–2875.
- (2) Zheng, H.; Yang, S. J.; Zheng, Y. C.; Cui, Y.; Zhang, Z.; Zhong, J. Y.; Zhou, J. Electrostatic Effect of Functional Surfaces on the Activity of Adsorbed Enzymes: Simulations and Experiments. *ACS Appl. Mater. Interfaces* **2020**, *12*, 35676–35687.
- (3) Pankratov, D.; Sotres, J.; Barrantes, A.; Arnebrant, T.; Shleev, S. Interfacial Behavior and Activity of Laccase and Bilirubin Oxidase on Bare Gold Surfaces. *Langmuir* **2014**, *30*, 2943–2951.
- (4) Jesionowski, T.; Zdarta, J.; Krajewska, B. Enzyme Immobilization by Adsorption: A Review. *Adsorption* **2014**, *20*, 801–821.
- (5) Schroeder, M. M.; Wang, Q.; Badieyan, S.; Chen, Z.; Marsh, E. N. G. Effect of Surface Crowding and Surface Hydrophilicity on the Activity, Stability and Molecular Orientation of a Covalently Tethered Enzyme. *Langmuir* **2017**, *33*, 7152–7159.
- (6) Jasensky, J.; Ferguson, K.; Baria, M.; Zou, X.; McGinnis, R.; Kaneshiro, A.; Badieyan, S.; Wei, S.; Marsh, E. N. G.; Chen, Z. Simultaneous Observation of the Orientation and Activity of Surface-Immobilized Enzymes. *Langmuir* **2018**, *34*, 9133–9140.
- (7) Badjić, J. D.; Kostić, N. M. Effects of Encapsulation in Sol-Gel Silica Glass on Esterase Activity, Conformational Stability, and Unfolding of Bovine Carbonic Anhydrase II. *Chem. Mater.* **1999**, *11*, 3671–3679.
- (8) Khaldi, K.; Sam, S.; Gouget-Laemmel, A. C.; Henry De Villeneuve, C.; Moraillon, A.; Ozanam, F.; Yang, J.; Kermad, A.; Ghellai, N.; Gabouze, N. Active Acetylcholinesterase Immobilization on a Functionalized Silicon Surface. *Langmuir* **2015**, *31*, 8421–8428.
- (9) Bhatia, S. K.; Cooney, M. J.; Shriver-Lake, L. C.; Fare, T. L.; Ligler, F. S. Immobilization of Acetylcholinesterase on Solid Surfaces: Chemistry and Activity Studies. *Sens. Actuators, B* **1991**, *3*, 311–317.

(10) Kastantin, M.; Faulón Marruecos, D.; Grover, N.; Yu McLoughlin, S.; Schwartz, D. K.; Kaar, J. L. Connecting Protein Conformation and Dynamics with Ligand-Receptor Binding Using Three-Color Förster Resonance Energy Transfer Tracking. *J. Am. Chem. Soc.* **2017**, *139*, 9937–9948.

(11) Love, J. C.; Estroff, L. A.; Kriebel, J. K.; Nuzzo, R. G.; Whitesides, G. M. Self-Assembled Monolayers of Thiolates on Metals as a Form of Nanotechnology. *Chem. Rev.* **2005**, *105*, 1103–1170.

(12) Bain, C. D.; Evall, J.; Whitesides, G. M. Formation of Monolayers by the Co-adsorption of Thiols on Gold: Variation in the Head Group, Tail Group, and Solvent. *J. Am. Chem. Soc.* **1989**, *111*, 7164–7175.

(13) Bain, C. D.; Whitesides, G. M. Modeling Organic Surfaces with Self-assembled Monolayers. *Angew. Chem.* **1989**, *1*, 110–116.

(14) Correira, J. M.; Webb, L. J. Formation and Characterization of a Stable Monolayer of Active Acetylcholinesterase on Planar Gold. *Langmuir* **2022**, *38*, 3501–3513.

(15) Gallardo, I. F.; Webb, L. J. Demonstration of α -Helical Structure of Peptides Tethered to Gold Surfaces Using Surface Infrared and Circular Dichroic Spectroscopies. *Langmuir* **2012**, *28*, 3510–3515.

(16) Ellman, G. L. Tissue Sulfhydryl Groups. *Arch. Biochem. Biophys.* **1959**, *82*, 70–77.

(17) Tompkins, H. G.; Hilfiker, J. N. *Spectroscopic Ellipsometry: Practical Application to Thin Film Characterization*; Momentum Press, 2016.

(18) De Feijter, J. A.; Benjamins, J.; Veer, F. A. Ellipsometry as a Tool to Study the Adsorption Behavior of Synthetic and Biopolymers at the Air-Water Interface. *Biopolymers* **1978**, *17*, 1759–1772.

(19) Zhao, H.; Brown, P. H.; Schuck, P. On the Distribution of Protein Refractive Index Increments. *Biophys. J.* **2011**, *100*, 2309–2317.

(20) Felder, C. E.; Prilusky, J.; Silman, I.; Sussman, J. L. A Server and Database for Dipole Moments of Proteins. *Nucleic Acids Res.* **2007**, *35*, 512–521.

(21) Yang, S.; Liu, J.; Zheng, H.; Zhong, J.; Zhou, J. Simulated Revelation of the Adsorption Behaviours of Acetylcholinesterase on Charged Self-Assembled Monolayers. *Nanoscale* **2020**, *12*, 3701–3714.

(22) Chen, X.; Ferrigno, R.; Yang, J.; Whitesides, G. M. Redox Properties of Cytochrome c Adsorbed on Self-Assembled Monolayers: A Probe for Protein Conformation and Orientation. *Langmuir* **2002**, *18*, 7009–7015.

(23) Vogler, E. A. *Surface Modification for Biocompatibility*; Elsevier: Boston, MA 2013, DOI: 10.1016/B978-0-12-415995-2.00008-8.

(24) Mrksich, M.; Sigal, G. B.; Whitesides, G. M. Surface Plasmon Resonance Permits In Situ Measurement of Protein Adsorption on Self-Assembled Monolayers of Alkanethiolates on Gold. *Langmuir* **1995**, *11*, 4383–4385.

(25) Roach, P.; Farrar, D.; Perry, C. C. Interpretation of Protein Adsorption: Surface-Induced Conformational Changes. *J. Am. Chem. Soc.* **2005**, *127*, 8168–8173.

(26) Stadler, H.; Mondon, M.; Ziegler, C. Protein Adsorption on Surfaces: Dynamic Contact-Angle (DCA) and Quartz-Crystal Microbalance (QCM) Measurements. *Anal. Bioanal. Chem.* **2003**, *375*, 53–61.

(27) Arima, Y.; Iwata, H. Effect of Wettability and Surface Functional Groups on Protein Adsorption and Cell Adhesion Using Well-Defined Mixed Self-Assembled Monolayers. *Biomaterials* **2007**, *28*, 3074–3082.

(28) Johnson, K. A.; Goody, R. S. The Original Michaelis Constant: Translation of the 1913 Michaelis-Menten Paper. *Biochemistry* **2011**, *50*, 8264–8269.

(29) Hebditch, M.; Warwicker, J. Web-Based Display of Protein Surface and pH-Dependent Properties for Assessing the Developability of Biotherapeutics. *Sci. Rep.* **2019**, *9*, 1–9.

(30) Salgado, J. C.; Rapaport, I.; Asenjo, J. A. Is It Possible to Predict the Average Surface Hydrophobicity of a Protein Using Only Its Amino Acid Composition? *J. Chromatogr. A* **2005**, *1075*, 133–143.

(31) Yu, G.; Wu, W.; Zhao, Q.; Wei, X.; Lu, Q. Efficient Immobilization of Acetylcholinesterase onto Amino Functionalized Carbon Nanotubes for the Fabrication of High Sensitive Organophosphorus Pesticides Biosensors. *Biosens. Bioelectron.* **2015**, *68*, 288–294.

(32) Liu, J.; Yu, G.; Zhou, J. Ribonuclease A Adsorption onto Charged Self-Assembled Monolayers: A Multiscale Simulation Study. *Chem. Eng. Sci.* **2015**, *121*, 331–339.

(33) Xu, Z.; Yang, S.; Xie, Y.; Yu, H.; Zhou, J. Modulating the Adsorption Orientation of Methionine-Rich Laccase by Tailoring the Surface Chemistry of Single-Walled Carbon Nanotubes. *Colloids Surf., B* **2022**, *217*, No. 112660.

(34) Kao, P.; Parhi, P.; Krishnan, A.; Noh, H.; Haider, W.; Tadigadapa, S.; Allara, D. L.; Vogler, E. A. Volumetric Interpretation of Protein Adsorption: Interfacial Packing of Protein Adsorbed to Hydrophobic Surfaces from Surface-Saturating Solution Concentrations. *Biomaterials* **2011**, *32*, 969–978.

(35) Vogler, E. A. The Goldilocks Surface. *Biomaterials* **2011**, *32*, 6670–6675.

□ Recommended by ACS

Imaging Heterogeneous 3D Dynamics of Individual Solutes in a Polyelectrolyte Brush

Dongyu Fan, Christy F. Landes, *et al.*
JUNE 08, 2023
LANGMUIR

READ 

Zwitterionic Surface Modification of Aldehydated Sulfofobetaine Copolymers for the Formation of Bioinert Interfaces

Ying-Nien Chou and Ming-Zu Ou
JUNE 23, 2023
ACS APPLIED POLYMER MATERIALS

READ 

Interfacial Behavior of Cubosomes: Combined Langmuir-Blodgett/Langmuir-Schaefer and AFM Investigations

Michalina Zaborowska, Renata Bilewicz, *et al.*
MAY 25, 2023
LANGMUIR

READ 

Biomimetic Photo-Switches Softening Model Lipid Membranes

Jérémie Pecourneau, Andreea Pasc, *et al.*
DECEMBER 05, 2022
LANGMUIR

READ 

Get More Suggestions >